

Observation of two relaxation mechanisms in transport between spin-split edge states at high imbalance

E.V. Deviatov,¹ A. Wurtz,² A. Lorke,² M. Yu. Melnikov,¹ V.T. Dolgoplov,¹ D. Reuter,³ and A.D. Wieck³

¹Institute of Solid State Physics, Chernogolovka, Moscow District 142432, Russia

²Laboratorium für Festkörperphysik, Universität Duisburg-Essen, Lotharstr. 1, D-47048 Duisburg, Germany

³Lehrstuhl für Angewandte Festkörperphysik, Ruhr-Universität Bochum,

Universitätsstrasse 150, D-44780 Bochum, Germany

(dated: March 22, 2024)

Using a quasi-Corbino geometry to directly study electron transport between spin-split edge states, we find a pronounced hysteresis in the $I-V$ curves, originating from slow relaxation processes. We attribute this long-time relaxation to the formation of a dynamic nuclear polarization near the sample edge. The determined characteristic relaxation times are 25 s and 200 s which points to the presence of two different relaxation mechanisms. The two time constants are ascribed to the formation of a local nuclear polarization due to ip -op processes and the diffusion of nuclear spins.

I. INTRODUCTION

In a quantizing magnetic field, energy levels in a two dimensional electron gas (2DEG) bend up near the edges of the sample, forming edge states (ES) at the lines of intersection with the Fermi level. According to the picture of Buttiker¹, transport in two dimensional electron systems takes place mostly in ES because of a zero bulk dissipative conductivity in the quantum Hall effect regime. This single-particle picture was modified by Shklovskii et al.², taking into account electrostatic interactions between electrons. This leads to the appearance of a set of incompressible and compressible strips near the 2DEG edge. This ES picture is nowadays widely accepted and in good agreement with experimental results³.

Several experiments were performed, investigating not only transport along the 2DEG edge but also inter-edge-state charge transfer³. In charge transfer between the two spin-split ES of the lowest Landau level, the necessity for spin- ip s diminishes the tunneling probability. For this reason, the equilibration length between spin-split edge states can be as high as 1 μ m at low temperatures, despite the large spatial overlap of electron wave functions^{4,5}.

Formerly, the electron spin- ip was attributed to spin-orbit coupling^{5,6} while today it is known that the electron spin- ip can be accompanied by the spin-op of a nucleus (so-called dynamic nuclear polarization (DNP)) near the edge^{7,8,9}. A key feature of this effect is a pronounced hysteresis of the $I-V$ traces due to the high nuclear-spin-lattice relaxation time T_1 , which was also reported for the bulk^{10,11,12,13}.

Most experiments on the charge transfer between ES were performed using the so-called cross-gate technique¹⁴ where current is injected into one outer ES. The resistance of this outer ES reflects the current redistribution among all participating ES. To see a significant effect, the size of the interaction region has to be comparable with the equilibration length⁵. For this reason the cross-gate method is not suitable to study electron transport at high imbalance between ES with a negligible current between

them. On the other hand, new physical effects such as a hysteresis due to the switching of the positions of two ES¹⁵, are predicted in the regime of high imbalance.

Here we apply a quasi-Corbino geometry¹⁶ to study electron transport between spin-resolved ES at high imbalance. We find a pronounced hysteresis in the $I-V$ curves, originating from slow relaxation processes. We determine characteristic relaxation times to be 25 s and 200 s which points to the presence of two different relaxation mechanisms. These results are discussed in terms of the dynamic nuclear polarization of the edge region via the hyperfine interaction.

II. SAMPLES AND EXPERIMENTAL TECHNIQUE

The samples are fabricated from two molecular beam epitaxially-grown GaAs/AlGaAs heterostructures with different carrier concentrations and mobilities. One of them (A) contains a 2DEG located 70 nm below the surface. The mobility at 4K is 800 000 cm^2/Vs and the carrier density $3.7 \cdot 10^{11} \text{cm}^{-2}$. For heterostructure B the corresponding parameters are 110 nm, 2.2 $\cdot 10^6 \text{cm}^2/\text{Vs}$ and $1.35 \cdot 10^{11} \text{cm}^{-2}$. We obtain similar results on samples of both materials. For this reason we restrict the discussion here to results obtained from samples of wafer A.

Samples are patterned in a quasi-Corbino geometry¹⁶ (see Fig. 1). The square-shaped mesa has a rectangular etched region inside. Ohmic contacts are made to the inner and outer edges of the mesa. The top gate does not completely encircle the inner etched region but leaves uncovered a narrow (3 μ m) strip (gate-gap) of 2DEG at the outer edge of the sample.

In a quantizing magnetic field at integer filling factors (e.g. $\nu = 2$, see Fig. 1) edge channels are running along the etched edges of the sample. Depleting the 2DEG under the gate to a smaller integer filling factor (e.g. $\nu = 1$, as shown in the figure) some channels ($\nu = 1$) are reflected at the gate edge and redirected to the outer edge of the sample. In the gate-gap region, edge channels originate

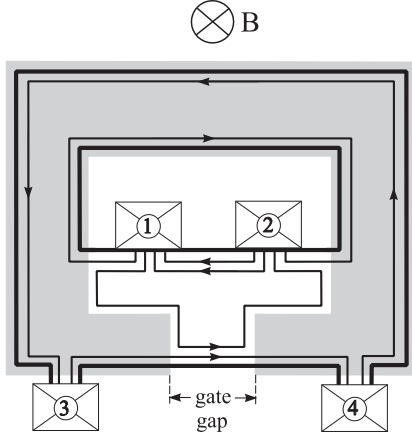


FIG. 1: Schematic diagram of the pseudo-Corbino geometry. Contacts are positioned along the etched edges of the ring-shaped mesa. The shaded area represents the Schottky-gate. Arrows indicate the direction of electron drift in the edge channels for the outlined configuration: filling factors are $\nu = 2$ in the ungated regions and $g = 1$ under the gate.

ing from different contacts run in parallel along the outer (etched) edge of the sample, on a distance determined by the gate-gap width. Thus, the applied geometry allows us to separately contact edge states and bring them into an interaction on a controllable length. A voltage applied between inner and outer ohmic contacts makes it possible to produce a significant imbalance between edge channels because the gate-gap width of a few microns is much smaller than the typical equilibration length between ES (more than 100 nm at low temperatures^{3,5,16}).

In our experimental set-up, a positive bias $V > 0$ moves the outer ES down in energy with respect to the inner one (see Fig. 2 b)) (one inner ohmic contact is grounded). Therefore, a small positive bias attenuates the edge potential profile between outer and inner edge states. At voltages close to the energy which separates the involved edge states, the potential barrier between edge states disappears and a significant current starts to flow^{7,16}. In contrast, a negative bias steepens the potential relief (see Fig. 2 c)), so that electrons at any negative bias have to tunnel through the magnetic-field induced barrier. Experimental $I-V$ traces are expected to be nonlinear and asymmetric with a characteristic onset voltage on the positive branch, roughly equal to the corresponding energy gap (for a more thorough discussion see¹⁶). A current in this case directly reflects a charge transfer between edge channels in the gate-gap in contrast to the conventional Hall-bar geometry with crossing gates⁵. Whereas, no clear onset behaviour can be seen for negative applied voltages.

Adjusting both, magnetic field B and gate voltage V_g , it is possible to change the number of ES in the gate-gap region (equal to the bulk filling factor ν) and – independently – the number g of ES transmitted under the gate. Thus the applied geometry allows us to study transport

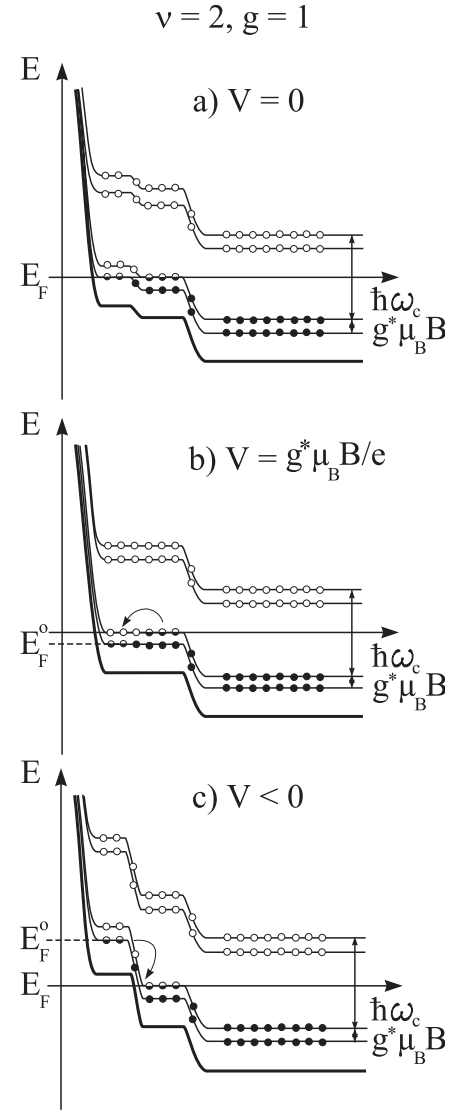


FIG. 2: Energy subband diagram of the sample edge in the gate-gap. a) No voltage V applied between inner and outer edge states. b) $V > 0$, in the situation shown, the outer edge state is shifted down in energy by $eV = g\mu_B$. The potential profile is attenuated between inner and outer edge states. c) $V < 0$, the energy shift is equal to $eV > 0$.

between spin-split or cyclotron-split edge channels depending on the adjusted filling factors ν and g .

We obtain $I-V$ curves from dc four-point measurements at a temperature of 30 mK in magnetic fields up to 16 T. The measured voltages V are always much smaller than the gate voltage, so the electron density under the gate is unchanged during the $I-V$ sweeps. The results presented in the paper are temperature independent below 0.5 K.

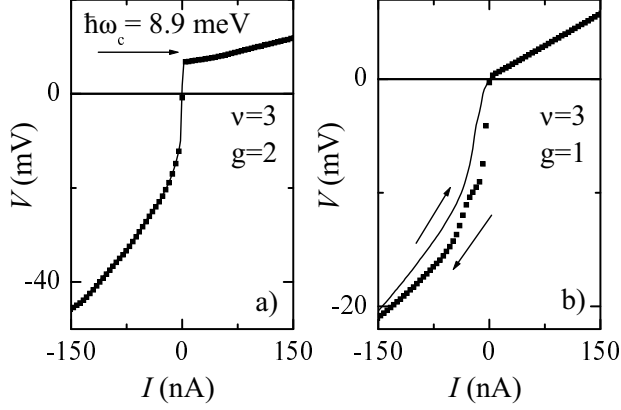


FIG. 3: I - V curves for filling factor combinations a) $\nu = 3; g = 2$ (cyclotron splitting) and b) $\nu = 3; g = 1$ (spin splitting). The solid line indicates a sweep from negative to positive currents and dots represent the reverse sweep direction. The arrow in a) denotes the theoretical value of the cyclotron gap, whereas the arrows in b) exhibit the sweep directions. For the dotted curves the number of points is reduced by 10 times for reasons of clarity. The magnetic field is 5.2 T.

III. EXPERIMENTAL RESULTS

A typical I - V curve is shown in Fig 3 a) for the filling factor combination $\nu = 3; g = 2$. The I - V trace reflects transport in the gate-gap between cyclotron-split edge states. It is strongly non-linear and asymmetric with a positive onset voltage close to the value of the cyclotron energy¹⁶. The negative branch of the trace changes its slope at a voltage also comparable to $\hbar\omega_c/e$, due to the crossing of the outer (partially filled) ES with the excited (empty) level in the inner one.

Figure 3 b) shows an I - V curve for the filling factor combination $\nu = 3; g = 1$ which corresponds to transport between spin-split ES. The onset voltage on the positive branch is much smaller in this case, because of the smaller value of the spin gap in comparison to the cyclotron gap. However, the most important difference from Fig. 3 a) is a large hysteresis for the negative branch of the I - V curve.

The curves in Fig. 3 are obtained by continuous sweep from positive to negative currents and vice versa. Increasing the sweep rate increases the hysteresis effect. This indicates that the hysteresis is the result of a long-time relaxation process with a characteristic time comparable to the sweep time of about ten minutes.

The described behaviour is contrary to the one observed for transport through the cyclotron splitting (see Fig. 3 a)) where there is no hysteresis effect discernible. Because of the much smaller bulk 2DEG dissipative conductivity under the gate for cyclotron splitting factors, the obtained hysteresis can not be caused by the charging of the bulk 2DEG. This fact was checked for different

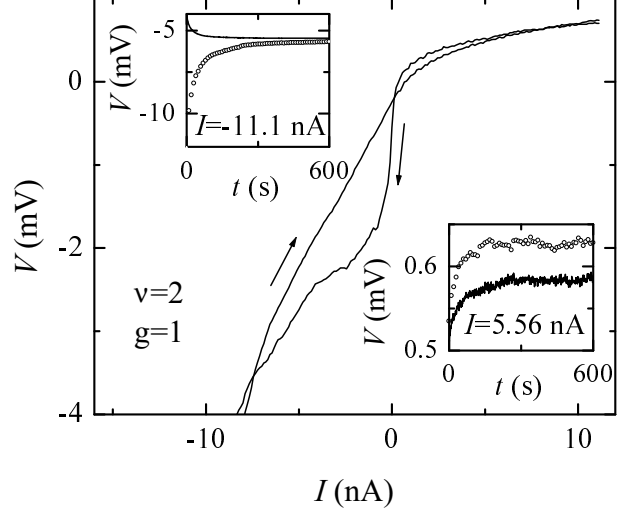


FIG. 4: I - V curves for the filling factor combination $\nu = 2; g = 1$ (spin splitting) for small biases. The two different sweep directions are indicated by arrows. Insets show the relaxation curves at fixed currents $I = -11.1$ nA (left inset) and $I = 5.56$ nA (right inset) obtained for two dwelling currents $I_{\text{dwell}} = -222$ nA (solid curves) and $I_{\text{dwell}}^+ = 111$ nA (dotted ones). The magnetic field is 7.7 T.

filling factor combinations on samples from two different wafers: the hysteresis is present only for transport between spin-split edge channels and there is no hysteresis in the I - V curves corresponding to cyclotron splitting.

The zero-bias region of the I - V trace is shown in Fig. 4 for the filling factor combination $\nu = 2; g = 1$. A small hysteresis can also be observed for the positive branch. The asymmetry of the I - V curve is also reflected in the hysteresis: at negative biases it is more pronounced, while for the positive branch there is only a small hysteresis observable at very small currents.

To directly investigate the time dependence of the relaxation, we measure the change of the voltage drop at different fixed currents. To prepare a stable state of the system, a dwelling current I_{dwell} is applied for a time long enough (about 10 minutes) to observe a stable voltage drop. This procedure provides a reproducible initial state of the system. Directly switching to a current I after the dwell, we measure the time-dependent voltage drop $V(t)$. The resulting $V(t)$ curves are well reproducible.

Examples of these $V(t)$ dependencies are shown in the insets of Fig. 4. For both, positive and negative branches of the I - V trace, time-dependent relaxation is measured after dwelling at two different currents $I_{\text{dwell}}^+ = 111$ nA (circles) and $I_{\text{dwell}} = -222$ nA (solid curves). It can be seen that both branches of the I - V traces differ not only in the size of the relaxation (by two orders of magnitude), but also in the dependence on the sign of the dwelling current. For the positive branch ($I > 0$) $V(t)$ curves are qualitatively independent of the sign of I_{dwell} and the

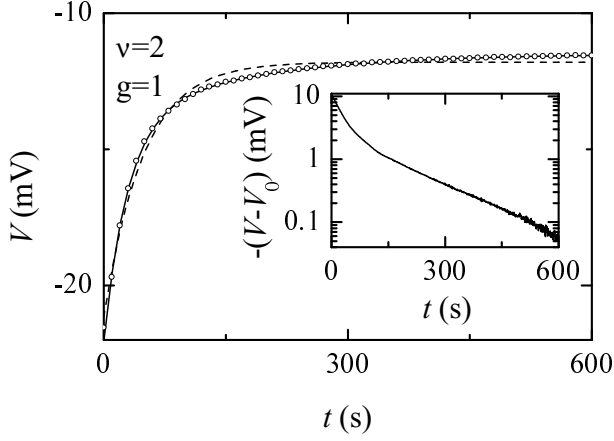


FIG. 5: Relaxation curve for the filling factor combination $\nu=2; g=1$ at $I = 22.2$ nA for a positive dwelling current $I_{\text{dwell}}^+ = 111$ nA (circles). The number of points is diminished by 10 times for clarity. The solid curve indicates a fit by a double exponential decay function (Eq. 1), the dashed one is a fit by one exponential function only. The inset shows the same experimental relaxation curve in a semi logarithmic plot shifted by $V_0 = V(t=1) = 11.5$ mV.

relaxation always appears as a rising of the resistance. For the negative branch ($I < 0$), on the other hand, the resistance is increasing with time for negative $I_{\text{dwell}}^- < 0$ and decreasing for a positive one $I_{\text{dwell}}^+ > 0$. Thus, for the negative branch of the $I-V$ trace the character of the relaxation as well as its starting value are very sensitive to the sign of I_{dwell} .

The experimental $V(t)$ curves seem to obey an exponential law of relaxation but clearly consist of two different regions. We find that the relaxation curves for transport between two spin-split edge channels at negative currents can well be fitted by a double-exponential decay

$$V(t) = V_0 + V_1 \exp\left(-\frac{t}{\tau_1}\right) + V_2 \exp\left(-\frac{t}{\tau_2}\right); \quad (1)$$

as shown in Fig. 5 (solid curve). For a comparison, a single-exponential fit (dashed curve in Fig. 5) is given, which cannot describe adequately the experimental data, especially for $t > 50$ s. The inset in semi logarithmic axes demonstrates clearly the presence of the second exponential dependence which especially dominates the long-time behavior.

The decay times obtained from the double-exponential fit are of the order of $\tau_1 \approx 25$ s and $\tau_2 \approx 200$ s. They are practically independent of the dwelling current and the measurement current. Measurements of the relaxation in tilted fields show that the time constants τ_1 and τ_2 are also independent of the in-plane magnetic field. For positive currents (positive branch of the $I-V$ trace) the accuracy of the determination of τ_2 is smaller than for

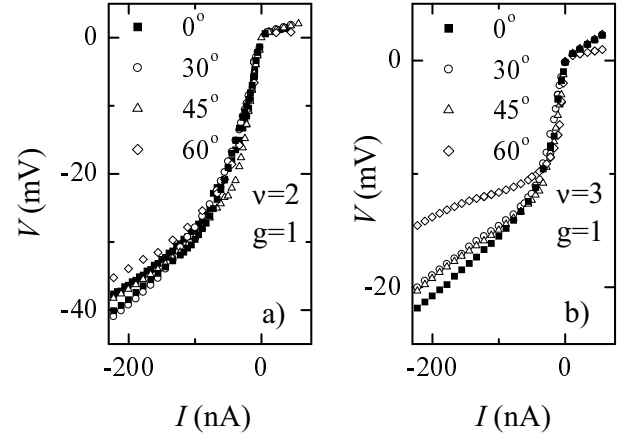


FIG. 6: Steady-state $I-V$ curves for normal and tilted magnetic fields for a) $\nu=2; g=1$ and b) $\nu=3; g=1$. The tilt angles shown are $0^\circ, 30^\circ, 45^\circ$, and 60° . For the filling factor combination $\nu=2; g=1$ at normal magnetic field the results of two different cooling cycles of the sample are presented.

negative ones because of the smaller value of the relaxation (see inset to Fig. 4).

From the $V(t)$ curves the time-independent, steady state of the system can be extrapolated. It can be obtained either from V_0 as a fitting parameter (see Eq. (1)) or as the last value of the relaxation curve at $t = 600$ s. The difference is negligible. The resulting steady state $I-V$ traces are presented in Fig. 6 for two different spin-split filling factor combinations for normal and tilted magnetic fields. It can be seen that the stationary $I-V$ curves for $\nu=2; g=1$ (Fig. 6 a)) are independent of the in-plane component of the magnetic field. The deviations are of the same order as the difference between two different cooling cycles at zero tilt angle.

For other spin-split filling factor combinations (such as $\nu=3; g=1$) a larger number of edge channels is involved in the transport. Besides charge transfer among spin-split ES in the gate-gap, transport between cyclotron-split edge channels has to be taken into account. The cyclotron-splitting is well known¹⁷ to be dependent on the in-plane magnetic field, which is also verified for this sample.

Therefore, there is some influence of the in-plane magnetic field observable on the steady-state $I-V$ traces (see Fig. 6 b)) for these filling factor combinations. The resistance is decreasing with increasing in-plane magnetic field because of the reduction of the cyclotron gap.

IV. DISCUSSION

For electron transfer between spin-resolved ES it is necessary to change both the spin and the spatial position of the electron. For this reason, we consider three pos-

sible mechanisms for the electron transfer: (i) magnetic impurities, (ii) spin-orbit interaction, and (iii) hyperfine interaction. An influence of the magnetic impurities can be excluded because of the high quality of the MBE process for GaAs/AlGaAs and taking into account the fact that our samples, which are grown in two different MBE systems, exhibit similar behavior.

The spin-orbit interaction is well known to be responsible for electron transfer between ES at small imbalance^{5,6}. It should also be taken into account for our samples, that some part of the electrons will relax in this way. However, spin-orbit coupling cannot explain a voltage relaxation on the macroscopic time scale of the order of $\tau_1 \approx 25$ s. The observed voltage relaxation is also independent of the in-plane magnetic field component, as both the relaxation times τ_1 ; τ_2 and the steady-state of the system are insensitive to the in-plane magnetic field. This is very unusual for the spin-orbit coupling and indicates a different origin of the relaxation for the transport between spin-resolved edge channels. On the other hand, the obtained relaxation time $\tau_1 \approx 25$ s is close to the nuclear spin relaxation times in GaAs (of the order of 30 s^{7,8}). For this reason, the relaxation can be attributed to the hyperfine interaction.

It is a well known fact that the hyperfine interaction in GaAs/AlGaAs heterostructures is strong enough to have an influence on transport experiments^{10,11,13}. A Hamiltonian of the hyperfine interaction can be written as

$$A \mathbf{I} \cdot \mathbf{S} = \frac{1}{2} (I^+ S^- + I^- S^+) + A S_z I_z; \quad (2)$$

where $A > 0$ is the hyperfine constant, \mathbf{I} is the nuclear spin and \mathbf{S} is the electron spin.

At the temperature of the experiment (30 mK) in a magnetic field (below 16 T) the static nuclear polarization $\hbar I_z$ by the external magnetic field is negligible. Nevertheless, a significant dynamic polarization of the nuclei is possible: an electron spin-flip causes the spin-flip of a nucleus in the GaAs lattice as described by the first term in Eq. 2 (the so called \mathbf{ip} -op process). Thus, a current

flow between spin-resolved edge channels produces a dynamic nuclear polarization (DNP) $\hbar I_z$ in the edge region of the sample^{7,8}. This polarization affects the electron energy through the second term in the Eq. 2 (the Overhauser shift). The influence of the nuclear polarization on the electron energy can be conveniently described by the effective Overhauser field $B_{OV} = A \hbar I_z / g_B$ which affects the Zeeman splitting $g_B (B + B_{OV})$.

A different relaxation behavior for positive and negative currents in our experiment can be qualitatively understood in terms of DNP. Let us discuss the filling factor combination $\nu = 2$; $g = 1$ (Fig. 2). Because of the negative effective g -factor ($g = -0.44$ in bulk GaAs), electron spins in the outer ES are polarized in the field direction ("up"-polarization) while in the inner ES they are polarized "down".

A negative applied bias shifts the outer ES up in energy with respect to the inner one (see Fig. 2 c)). Elec-

trons tunnel through the incompressible strip between outer and inner ES with a spin-flip from up to down. Some of these electrons relax due to the spin-orbit coupling, changing their energy by phonon emission. Nevertheless, inside the incompressible strip horizontal (in energy) transitions from the filled to empty states are possible due to the \mathbf{ip} -op process. The electron spin-flip from up to down leads to a nuclear spin-flip from down to up. Thus, a current persisting for a long time induces a DNP $\hbar I_z > 0$ in the gate-gap. Because of the negative g -factor in GaAs, the effective Overhauser field is antiparallel to the external field $B_{OV} < 0$ and decreases the value of the Zeeman splitting $g_B (B + B_{OV})$.

For a positive bias exceeding the onset voltage V_{on} g_B , there is no more potential barrier for electrons between edge states (see Fig. 2 b)). Electrons are flowing from the inner state to the outer ES and rotate the spin in vertical transitions afterwards (e.g. by emitting a photon), possibly far from the gate-gap region. Nevertheless, for a bias $V > 2V_{on}$ electrons can also tunnel from the filled (spin up) state to the empty one (spin down) in the incompressible strip due to the \mathbf{ip} -op mechanism, relaxing later to the ground state vertically. This \mathbf{ip} -op also produces an "up" nuclear polarization $\hbar I_z > 0$ in the gate-gap accompanied by an Overhauser field $B_{OV} < 0$ antiparallel to the external magnetic field, which diminishes the Zeeman splitting.

The value of the net nuclear polarization $\hbar I_z$ is therefore determined by the current connected with \mathbf{ip} -op processes which in turn is controlled by the applied bias V (see Fig. 2 c)). Thus, after dwelling at a positive current and switching to a negative one the nuclear polarization (i.e. the Overhauser field) is increasing significantly during the relaxation process, diminishing the Zeeman splitting. As the Zeeman splitting determines the spatial distance between spin-split ES, the tunneling length for the electrons decreases during the relaxation process⁸. For this reason, in the described situation, the relaxation goes along with a decrease of the resistance, as seen in the experiment (left inset to Fig. 4 (dots)).

Dwelling at a high negative current and switching to a lower one (i.e. closer to the zero), the nuclear polarization is diminishing in value. The corresponding change in the Overhauser field increases the Zeeman splitting. As a result, the tunneling length is rising, leading to an increase of the resistance, as depicted by the solid curve in the left inset to Fig. 4.

After a dwell at a negative or large positive current and switching to a small positive one, the nuclear polarization is always diminishing in value, leading to an increase of the resistance, as can be seen in the right inset to Fig. 4.

The proposed picture is thus in qualitative agreement with the experimental data. The relaxation should take place on a time scale determined by the nuclear spin-lattice relaxation time T_1 and obey an exponential law.

The presence of the two different relaxation times in the experimental traces can result directly from the injection of spin-polarized electrons in the gate-gap region

of the applied experimental geometry (Fig. 2, for a model calculation of a similar problem see¹⁸). The characteristic time scale for establishing the Overhauser field in the gate-gap is governed by the applied current and the diffusion of the nuclear polarization from the gate-gap region because of nuclear spin-spin interactions. A combination of these two processes should be responsible for the first relaxation with the characteristic time $\tau_1 \approx 25$ s. However, diffusion takes place on length scales much larger than the gate-gap width but smaller than the sample size. The second relaxation process with the characteristic time τ_2 of the order of the nuclear spin-lattice relaxation time T_1 is therefore attributed to the establishing of a stable nuclear polarization outside the gate-gap.

For measurements at constant current the relaxation in voltage reflects not only the change of the spatial positions of spin-split ES, but also directly the Overhauser shift. The latter is negligible for the strong relaxation at negative biases, but becomes significant for positive ones. From the value of the relaxation in this case we can estimate the Overhauser shift $A\hbar\gamma_z\hbar S_z i$ $V^+ \approx 100$ V, which gives a value of the Overhauser field $B_{OV} = V^+/(g\mu_B) \approx 4$ T. This value is smaller than the highest Overhauser field (5.3 T) reported for GaAs¹⁹ and close to the value reported for DNP in heterostructures⁷. On the other hand, $B_{OV} = 4$ T is strong enough to significantly change the Zeeman splitting in the external field of 7.7 T (which corresponds to $\mu_B = 2$ in the bulk) which gives further support for the proposed picture.

V. CONCLUSION

Performing direct measurements of the electron transport between spin-split edge states at high imbalance, we

found a long-time relaxation in contrast to charge transfer between cyclotron-split edge states. The determined characteristic times are of the order of 25 s and 200 s which points to the presence of two different relaxation mechanisms. We attribute this relaxation to the formation of a dynamic nuclear polarization (DNP) near the sample edge. The presence of the two relaxation mechanisms is interpreted as the formation of a DNP inside the gate-gap region due to flip-flop processes and outside it as a consequence of the diffusion of nuclear spins. We also found that an in-plane magnetic field has no influence both on the relaxation between two spin-split edge channels and on the steady-state of the system.

Acknowledgments

We wish to thank Dr. A. A. Shashkin for help during the experiments and discussions. We gratefully acknowledge financial support by the Deutsche Forschungsgemeinschaft, SPP "Quantum Hall Systems", under grant LO 705/1-1. The part of the work performed in Russia was supported by RFBR, the programs "Nanostructures" and "Mesoscopies" from the Russian Ministry of Sciences. V. T. D. acknowledges support by A. von Humboldt foundation.

dev@issp.ac.ru

- ¹ M. Büttiker Phys. Rev. B 38, 9375 (1988).
- ² D. B. Chklovskii, B. I. Shklovskii, and L. I. Glazman Phys. Rev. B 46, 4026 (1992).
- ³ For a review see R. J. Haug Semicond. Sci. Technol. 8, 131 (1993).
- ⁴ A. A. Shashkin, V. T. Dolgoplov, G. M. Gusev, Z. D. Kvon, JETP Lett., 53, 461 (1991).
- ⁵ G. Müller, D. Weiss, A. V. Khaetskii, K. von Klitzing, S. Koch, H. Nickel, W. Schlapp, and R. Lsch Phys. Rev. B 45, 3932 (1992).
- ⁶ A. V. Khaetskii Phys. Rev. B 45, 13777 (1992).
- ⁷ David C. Dixon, Keith R. Waldi, Paul L. McEuen and M. R. Melloch Phys. Rev. B 56, 4743 (1997).
- ⁸ T. Machida, S. Ishizuka, T. Yamazaki, S. Komiyama, K. Muraki and Y. Hirayama Phys. Rev. B 65, 233304 (2002).
- ⁹ Tomoki Machida, Tomoyuki Yamazaki, and Susumu Komiyama Applied Physics Letters 80, 4178 (2002).
- ¹⁰ M. Döbers, K. v. Klitzing, J. Schneider, G. Weimann, and K. Ploog Phys. Rev. Lett. 61, 1650 (1988).
- ¹¹ A. Berg, M. Döbers, R. R. Gerhardts, and K. v. Klitzing, Phys. Rev. Lett. 64, 2563 (1990).
- ¹² B. E. Kane, L. N. Pfeiffer, and K. W. West Phys. Rev. B 46, 7264 (1992).
- ¹³ W. Desrat, D. K. Maude, M. Potemski, J. C. Portal, Z. R. Wasilewski, and G. Hill Phys. Rev. Lett. 88, 256807 (2002).
- ¹⁴ R. J. Haug, A. H. MacDonald, P. Streda, and K. von Klitzing Phys. Rev. Lett. 61, 2797 (1988).
- ¹⁵ Lex Rijkels and Gerrit E. W. Bauer Phys. Rev. B 50, 8629 (1994).
- ¹⁶ A. Wurtz, R. Wildfeuer, A. Lorke, E. V. Deviatov, and V. T. Dolgoplov Phys. Rev. B 65, 075303 (2002).
- ¹⁷ J. J. Koning, R. J. Haug, H. Sigg, K. von Klitzing, and G. Weimann Phys. Rev. B 42, 2951 (1990). Our measurements of the onset voltage for the positive branch at cyclotron splitting factor combinations will be published elsewhere.
- ¹⁸ Yu. V. Pershin, S. N. Shevchenko, I. D. Vagner, and P. Wyder Phys. Rev. B 66, 035303 (2002).

- ¹⁹ D . Paget, G . Lampel, B . Sapoval, and V . S . Safarov, Phys. Rev. B 15, 5780 (1977).